Scientia Iranica F (2019) 26(6), 3938–3945

Sharif University of Technology
Scientia Iranica
Transactions F: Nanotechnology
http://scientiairanica.sharif.edu

Research Note

Fabrication of single-phase superparamagnetic iron oxide nanoparticles from factory waste soil

M. Karimipour*, N. Moradi, M. Molaei, and M. Dargahzadeh

Department of Physics, Vali-e-Asr University of Rafsanjan, Rafsanjan, P.O. Box 77139-6417, Iran.

Received 5 October 2018; received in revised form 9 March 2019; accepted 28 May 2019

KEYWORDS
Superparamagnetics;
Nanoparticles;
Oxygen cleaving method;
Iron (III) oxide;
Waste soil.

Abstract. The application of Iron (III) oxide nanoparticles in biology and medicine is much more than that of other magnetic nanoparticles. Biocompatibility with human body, stability, and ease of production are the main reasons for its considerable development during these years. In this study, single-phase iron (III) oxide nanoparticles were synthesized using factory waste soil instead of feedstock by the low-temperature wet chemical oxygen cleaving method. Using factory waste soil as the precursor material (feedstock) made the method cost-effective and innovative. In this synthesis method, single-phase iron (III) oxide was obtained by acid digestion of waste soil. The nanoparticles were analyzed by Fourier transform infrared spectroscopy (FTIR) and X-Ray Diffraction (XRD). The crystallite size of nanoparticles was calculated by XRD peaks through Debye-Scherrer formula at 11 nm. Transmission Electron Microscopy (TEM) images showed the spherical shape of nanoparticles with average size of 10 nm. Vibrating Sample Magnetometery (VSM) analysis was applied to determining the magnetic saturation and the size of nanoparticles, which was estimated at 9 nm. FTIR showed atomic bond between iron and oxygen (Fe-O) in nanoparticles. The results of XRD showed that the synthesized sample was cubic-spinel single-phase.

1. Introduction

In the last decade, nanotechnology has been developed considerably for fabrication, recognition, and special designing. Also, the properties of nanoparticles have been improved for medical applications and medical recognition. Fe_3O_4 or Magnetite is the most famous and developed magnetic nanoparticle due to its inertness, biocompatibility, chemical and physical stability, and ease of preparation [1]. Magnetic nanoparticles, as a group of nanoscale materials, brought a big revolution in recognition and curing methods in medical science. Magnetic nanoparticles less than 10 nm in the presence of an external magnetic field have extensively been used to enhance image clarity in Magnetic Resonance Imaging (MRI) [2,3]. In addition to medical recognition, nanoparticles are used in various curing methods, e.g., targeted drug delivery, transmission of gene, magnetic separation of materials, and tissue engineering [4-6].

Iron oxide consists of various compounds and each compound has different magnetic properties. Among them, the most favorable materials with significant magnetic properties are γ-Fe_2O_3, Fe_3O_4, and Fe_2O_3MO (M can be replaced with Mn, Co, Ni, and Cu). These materials possess the characteristic of ferromagnetism. Ferrimagnetism oxides by nature show lower magnetic reaction, but higher resistance to

*. *Corresponding author.*
E-mail address: m.karimipour@vru.ac.ir (M. Karimipour)

doi: 10.24200/sci.2019.51960.2448

oxidation than ferromagnetism materials such as Fe, Co, and Ni. Also, they have high stability in magnetic properties [5]. Ferrites are intricate magnetic oxides produced from iron (III) oxide as a basic component. They are soft materials which have had many applications during the last half century [7,8]. Magnetites (Fe_3O_4) and Maghemites (γ-Fe_2O_3) are the most common ferrites for making ferrofluid in the research in this area. Magnetite is a ferromagnetic material with reciprocal spinel structure. Magnetite, with the chemical formula of Fe_3O_4, is an iron oxide having the unit cell of 730 $Å^3$ with 8 molecules of Fe_3O_4, in which oxygen makes closed face-centered cubic (fcc) structure and Fe cations occupy interstitial tetragonal and octahedral sites [9,10]. Iron oxide nanoparticles are synthesized through various methods including Co-Precipitation and Hydrothermal methods, sol-gel, and combustion processes [11-13]. The main drawback of these methods is the need for expensive inorganic manufactured materials or particles during the oxidation process at high temperatures. Nowadays, development of novel methods that are easy and proper to large scales is a significant challenge [14]. Physical methods such as lithography, electron beam, etc. are not able to control the size of nanoparticles in nanometer limits [1]. On the other hand, chemical methods, such as chemical precipitation, are low-cost and require short processing time. Moreover, they have higher efficiency than the mentioned methods and allow controlling morphology, size, and distribution of nanoparticles.

Dhyvia et al. (2016) fabricated magnetite nanoparticles (Fe_3O_4) by using an aqueous solution containing iron ions in an alkaline medium and polyethylene glycol as a surfactant. Also, in the synthesis of iron oxide nanoparticles, chitosan thin layer as a surfactant was used [15]. Chaki et al. [16] and Khoshnevisan et al. in 2012 [17] reported the synthesis of magnetic iron oxide Fe_3O_4 nanoparticles by using CTAB as a surfactant. The results showed that the alternation of CTAB would decrease the size and increase the scattering of particles in solution, effectively, with no changes in superparamagnetic properties.

2. Material

Waste soil was provided by a Cu leaching factory in Rafsanjan, Iran. Sulfuric acid (H_2SO_4), phosphoric acid 85% (H_3PO_4), sodium hydroxide (NaOH), Cetyl Trimethyl Ammonium Bromide (CTAB), distilled water (H_2O), and acetone were purchased from Merck Co.

3. Synthesis process of iron oxide nanoparticles through wet chemical method

First, 0.2 g copper factory waste soil was dissolved in 40 ml sulfuric acid (phosphoric acid) and the solution was stirred for 3 hours by a magnetic stirrer until complete dissolving. Afterwards, 150 ml deionized water was slowly added to the solution. The solution was filtered once to became clear. In the next stage, the final solution was poured into three-neck round-bottom flasks in 45°C oil bath for one hour by oxygen cleaving, simultaneously. At this stage, no change in color was observed. Then, a proper volume of 10 M Sodium hydroxide solution was prepared and injected using a syringe until the solution became dark and pH was adjusted to 12. The dark precipitate was extracted from the solution using a simple magnet, washed twice with deionized water, and dried at room temperature. The final product was a 0.15 g black or brownish powder of Fe_3O_4. To prepare a sample with CTAB as surfactant for the sake of comparison, after filtering the dissolved soil, 0.02 g pre-dissolved CTAB in 50 ml DI water was added to it and then, the mixture was set for oxygen cleavage. Figure 1 shows the wet chemical oxygen cleaving synthesis method for nanoparticles.

4. Experimental characterization of nanocomposites

Energy Dispersive X-ray spectroscopy and Field Emission Scanning Electron Microscopy (EDX-FESEM) were performed by a Zeiss (Gemini 1550) microscope having a Field Emission (FE) electron source and an in-lens detector for secondary electrons and elemental

Figure 1. Setup of the synthesis of iron oxide nanoparticles by the wet chemical oxygen cleaving method and the resultant Fe_3O_4 dark precipitate.

mapping. Furrier Transformed Infra-Red (FTIR) data were collected using an AVATAR-370-FTIR THERMONICOLET spectrometer under two separate procedures. Crystalline structure of the powders was recorded by D8-Advance Bruker X-ray diffractometer (XRD) using Cu-Kα radiation with 1.54 Å wavelength. Scanning Electron Microscope (SEM) images were obtained using LEO 1450 VP system. For the magnetization curve, we used VSM 7400 Lake Shore. TEM and SAED images were recorded by Zeiss EM900 Transmission Electron Microscope.

5. Results and discussion

Energy-Dispersive X-ray (EDX) spectroscopy is an analytical method for quantitative analysis of elements as well as structural and chemical composition of the samples. To check the elemental composition of the soil and the prepared sample, EDX spectra are plotted in Figures 2 and 3, respectively. Spectra show that the waste soil comprises various impurities such as Fe, Cu, Zn, and Cr. However, as shown in Figure 3, only the peaks of Fe and Cu remain after F_3O_4 preparation, while the concentration of Cu is less than 5%.

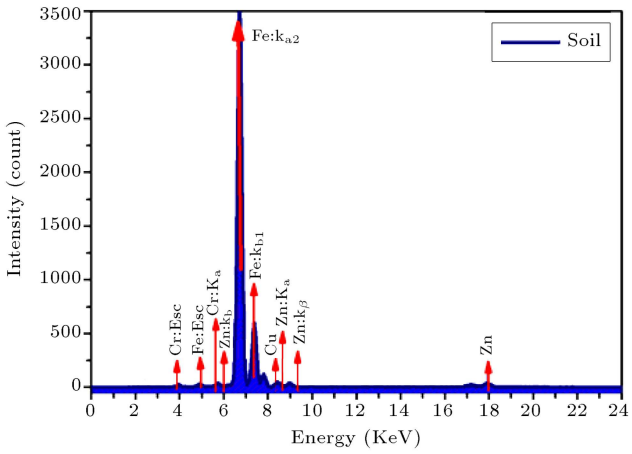

Figure 2. EDX spectrum of the initial waste soil.

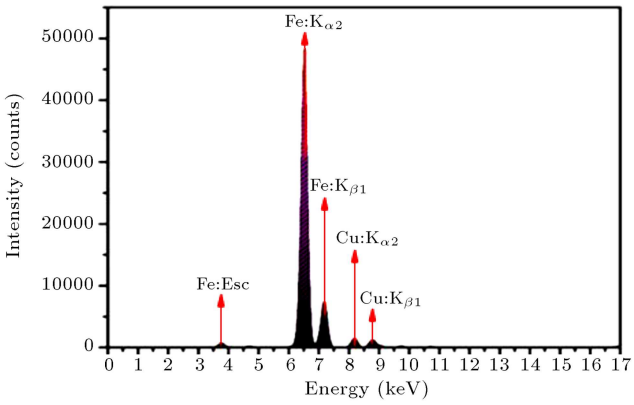

Figure 3. EDX spectrum of the synthesized sample without CTAB.

To identify the presence of molecular bonds of oxygen with iron and other possible bonds in the synthesized sample, FTIR spectroscopy was performed in the wavelength range of 400 cm^{-1} to 4000 cm^{-1}.

Figure 4 represents the FTIR spectroscopy of (a) waste soil and (b) the synthesized sample without CTAB surfactant as well as (c) a sample synthesized with CTAB. With due attention to spectroscopy graphs, the peaks can be classified in this way: those between 590 cm^{-1} and 1650 cm^{-1} are related to Fe-O [11,18] and those from 3200 to 3600 cm^{-1} are attributed to symmetrical and anti-symmetrical vibration-strain modes of O-H band. The latter implies physical absorption of water molecules in the air on the surface.

Figure 5(a) shows the XRD of the sample synthesized without CTAB and the crystal phases of waste soil. The waste soil with diffraction peaks of various compounds such as Cu, CuO, Fe_2O_3 and Fe_3O is presented in comparison with standard patterns (Cubic Fe_3O_4: JPCD-00-002-1035, Cubic Fe_2O_3: JPCD-00-002-1047, monoclinic CuO: JPCD-00-001-1117, Cu-

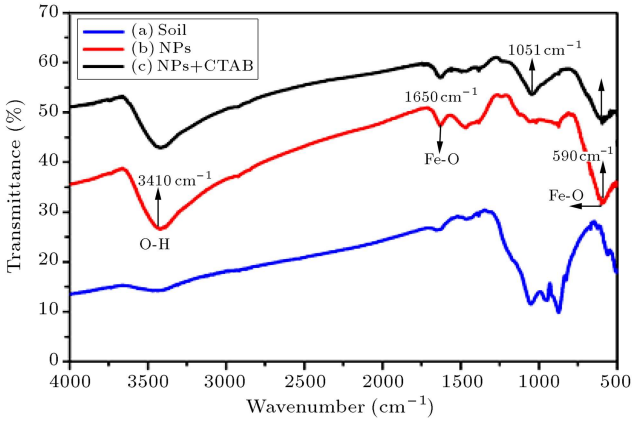

Figure 4. FTIR spectra of (a) the initial soil and the samples, (b) Fe_3O_4 synthesized without CTAB, and (c) Fe_3O_4 synthesized with CTAB.

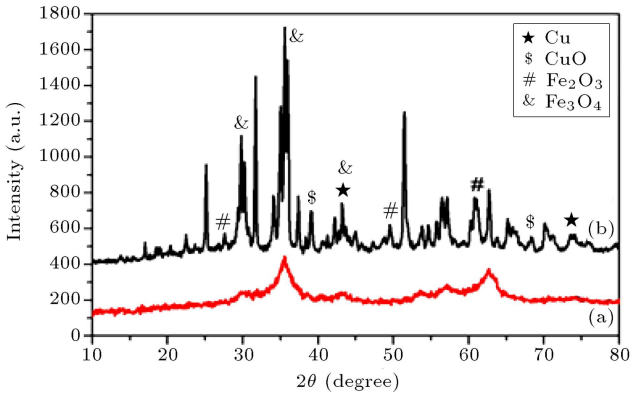

Figure 5. XRD patterns of (a) iron (III) oxide nanoparticles prepared without CTAB and (b) initial factory waste soil.

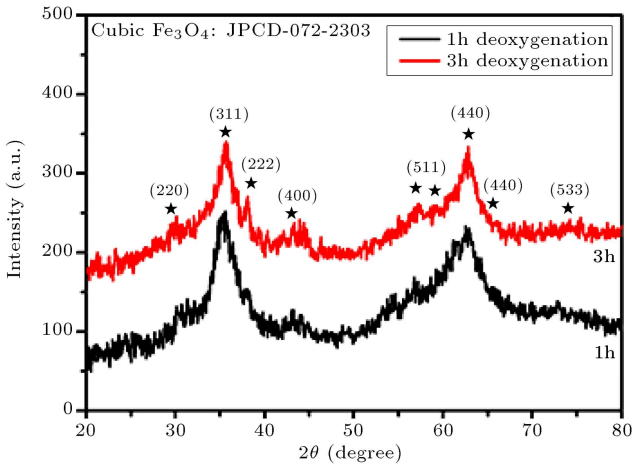

Figure 6. XRD patterns of nanoparticles at different times (1 h and 3 h) of oxygen cleaving process.

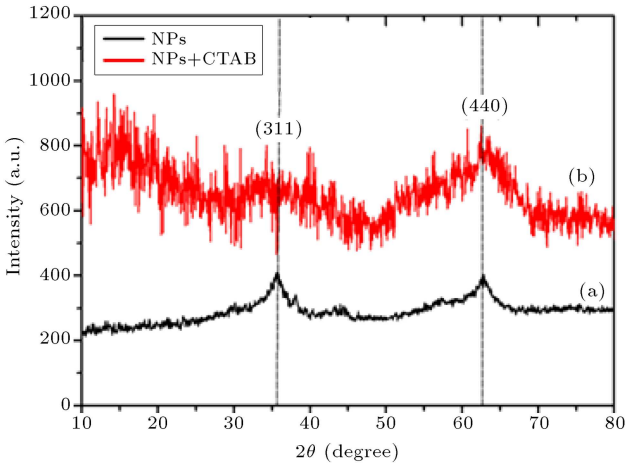

Figure 7. XRD patterns of synthesized samples: (a) Without CTAB as surfactant and (b) by adding 0.02 g of CTAB as surfactant.

bic Cu: JPCD-00-003-1005). The sample diffraction pattern of Figure 5(a) is endorsing the single phase magnetite with spinel cubic (Cubic Fe_3O_4: GPCD-01-075-1372).

Figure 6 shows the XRD pattern of iron (III) oxide nanoparticles (magnetite Fe_3O_4), which were synthesized in different treatment times (1 h and 3 h) using a single acid (sulfuric acid). The synthesis process was performed at 40°C. The proportion intensities of all diffracted peaks were reported with magnetic ferrite in spinel structure with Fd_3M space group and great consistency with Cubic Fe_3O_4: JPCD-072-2303. The six peaks in XRD of iron (III) oxide nanoparticles were related to lattice planes (220), (311), (400), (511), (440), (422), and (533) and consistent with spinel cubic structure.

The crystallite size of micro lattice could be calculated by XRD peaks and Debye-Scherrer formula (Eq. (1)) [19,20]. Sharp peaks showed well crystallization of nanoparticles. The intensity of (311) with ($2\theta = 51.35°$) degrees peak in XRD pattern, which is the sharpest peak, shows lattice growth in the privileged direction (311). The size of crystallite is 11 nm.

$$D = \frac{0.9\lambda}{\beta \cos\theta}. \quad (1)$$

D is the diameter of the crystal, β is the FWHM, and λ is the X-ray wavelength (0.154 nm) [20].

XRD pattern of iron oxide (Fe_3O_4) with CTAB as surfactant is shown in Figure 7. XRD pattern of Fe_3O_4 with CTAB surfactant indicates a weak crystal structure, which cannot be analyzed because of the very small size of particles. However, there is no change in the position of peaks, which shows that the synthesis process with CTAB surfactant makes no change in the phase of the Fe_3O_4 magnetic nanoparticles [17].

Figure 8 shows the images of scanning electron microscopy with different magnifications (a) with CTAB and (b) without CTAB. As observed in the images, the synthesized particles are spherical and the sizes are about 37.6 to 77.8 nanometers, respectively.

Chemical compound, cation distribution, and average size of iron oxide seeds affect the magnetic properties. The distribution of cations in tetragonal and octahedral positions predicates ferromagnetism, anti-ferromagnetism, and para-magnetism [10,21].

Magnetic hysteresis curves of iron (III) oxide superparamagnetic nanoparticles at room temperature with different times of oxygen cleaving (1 and 3 hours, zero and 30 mins) and synthesized samples with CTAB as surfactant and without CTAB are presented in Figure 9. All the samples show superparamagnetic behavior, because the coercive field in response to the external field is zero and the curve form is like the letter S.

The amount of magnetization of iron (III) oxide in oxygen cleaving for 3 h is 24 emu/g as computed in the intersection of magnetization axis versus $1/H^2$. Its difference in saturated magnetization range shows that time duration affects the size of nanoparticles. The decrease in saturated magnetization in comparison with the bulk and superparamagnetics synthesized using industrial precursors may be due to the decrease in the seed size as well as lattice and shape anisotropy [22,23]. In addition, the surface effects can decrease magnetization, because when particle size becomes smaller, the number of surface atoms would be increased. Consequently, the magnetic moment of surface atoms may be random in this surface area, so-called dead area, and lead to lower saturated magnetization [10,24]. Another reason for decrease in magnetization may be the slight changes in ferrite cation distribution. To estimate the magnetization moment of iron oxide nanoparticles, the following formula is used:

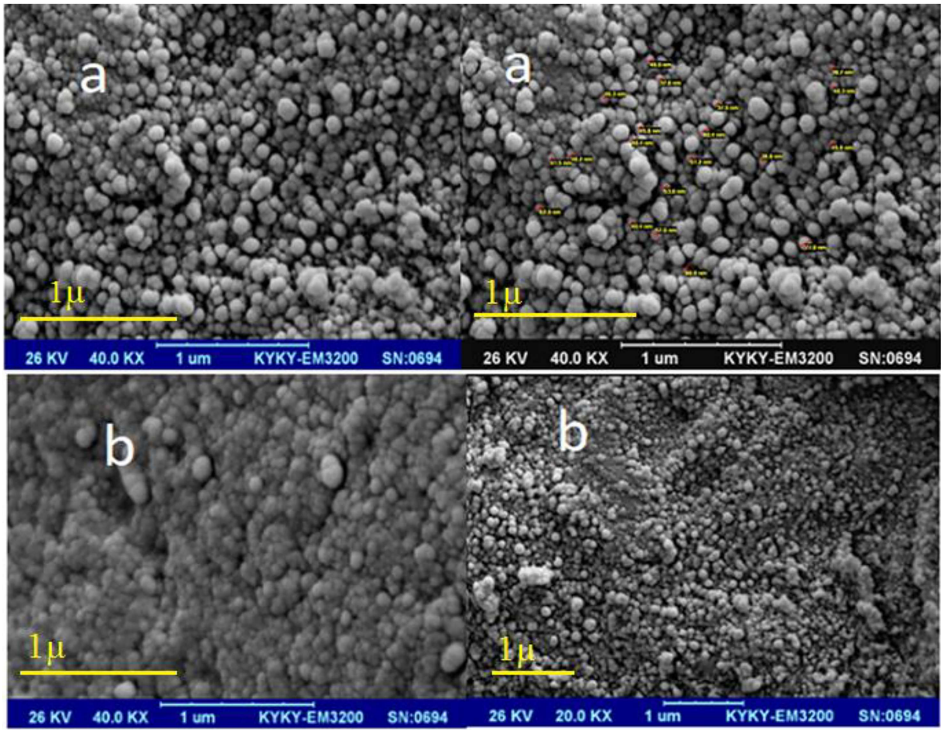

Figure 8. SEM images of iron (III) oxide nanoparticles synthesized: (a) With CTAB and (b) without CTAB.

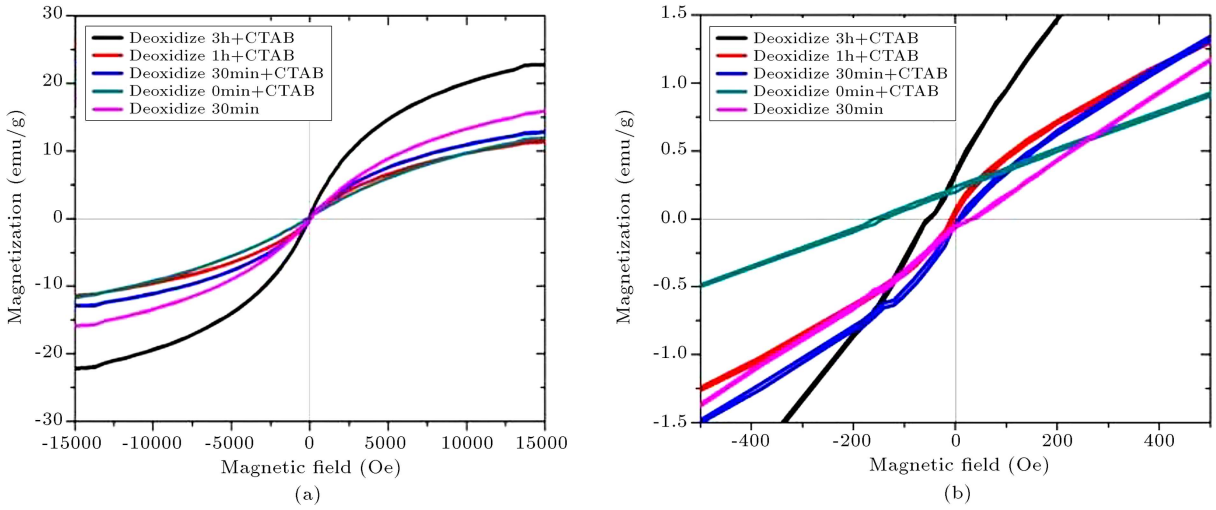

Figure 9. Magnetization curve of iron (III) oxide supermagnetic nanoparticles at different times of oxygen cleaving with the effect of CTAB surfactant: (a) In the range of −15000 to 15000 Oe and (b) in the range of −500 to 500 Oe.

$$d_m = \left[\frac{18K_BTx_i}{\pi\rho M_S^2}\right]^{1/3}, \tag{2}$$

where K_B is Boltzman constant, x_i represents magnetic susceptibility, M_s stands for magnetic saturation, and ρ represents density of nanoparticles (5.18 g/cm^3) [25-28]. The results of our calculations are given in Table 1. The size of nanoparticles was estimated at 9 nm, which is approximately equal to the size obtained by TEM. The average size of nanoparticles is smaller than the estimated crystallite size by XRD, which shows the existence of dead surface area in magnetic nanoparticles.

Figure 10 shows TEM images of iron (III) oxide nanoparticles. It shows the spherical shape of nanoparticles with the average size of 10 nm, which is very consistent with XRD and VSM results. The very small formation and superparamagnetic behavior of particles indicate that this method is a useful and industrial one for direct production of Fe_3O_4 nanoparticles from mineral sources available in soil.

In Figure 11, Selected Area (Electron) Diffrac-

Table 1. Magnetic characteristics obtained by the VSM analysis.

	M_r (emu/g)	M_s (emu/g)	x_i (emu/gOe)	H_c (Oe)	d_m (nm)
Deoxidization in 3 h+CTAB	0.33	22.7797	0.00476	0	9.85
Deoxidization in 1 h+CTAB	0.045	11.37221	0.00222	0	9.63
Deoxidization in 30 min+CTAB	0.039	12.76989	0.00251	0	9.65
Deoxidization in 0 min+CTAB	0.215	11.89195	0.00134	0	8.02
Deoxidization in 30 min	0.055	15.94361	0.00229	0	8.69

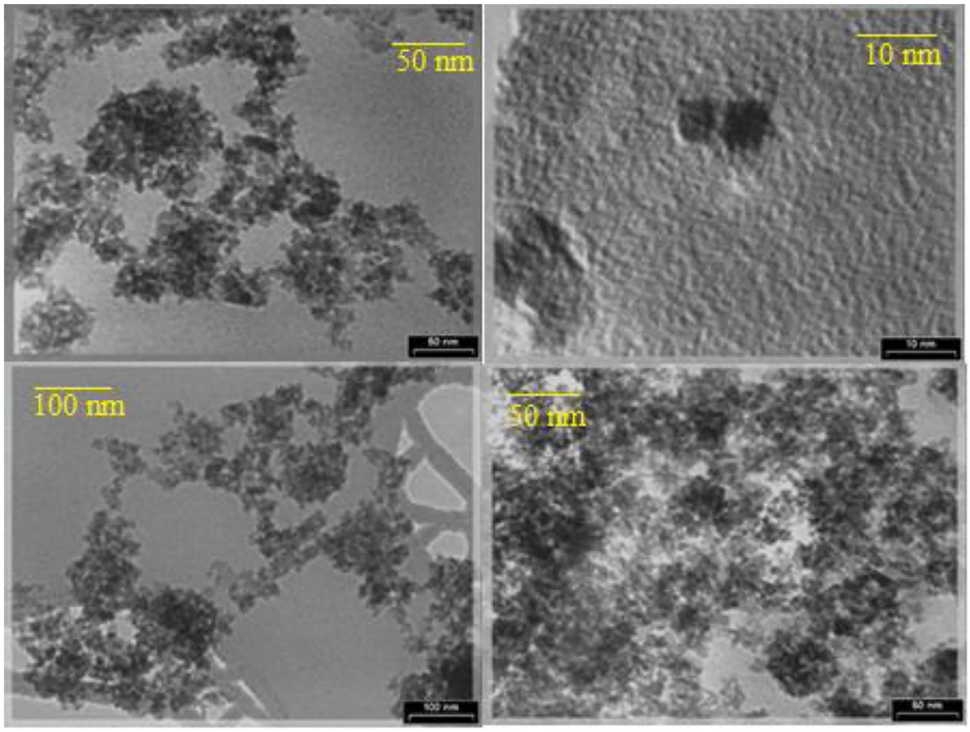

Figure 10. TEM images of iron oxide nanoparticles synthesized without CTAB at different scales.

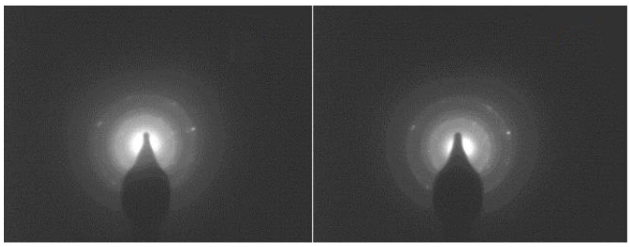

(a) (b)

Figure 11. SAED patterns of iron (III) oxide nanoparticles synthesized: (a) With CTAB and (b) without CTAB.

tion (SAED) pattern is shown for samples (a) with and (b) without CTAB. Dispersion of light points in rings and the stability of points prove the single-crystal nanoparticles. Moreover, they show that the nanoparticles are well crystallized even in the absence of CTAB as stabilizer. Thus, this method can also be developed for the preparation of Fe_3O_4 nanoparticles with superparamagnetic behavior without the need for surfactant [29,30].

6. Conclusion

In this study, single-phase iron (III) oxide was synthesized from factory waste soil as precursor by means of the wet chemical oxygen cleaving method at room temperature. Considering the fact that the primary material was factory waste soil (feedstock), the method can be considered as an economically cost-effective as well as innovative one. The particles showed superparamagnetic behavior at room temperature with sizes of about 10 nm, as estimated from the TEM images as well as XRD and VSM analyses.

Acknowledgement

This work was supported by Vali-e-Asr university of Rafsanjan.

References

1. Gupta, A.K. and Gupta, M. "Synthesis and surface engineering of iron oxide nanoparticles for biomedical applications", *Biomaterials*, **26**(18), pp. 3995-4021 (2005).
2. Ansari, S.A., Ficiarà, M.K., Ruffinatti, F.A., et al. "Magnetic iron oxide nanoparticles: Synthesis, characterization and functionalization for biomedical applications in the central nervous system", *Materials*, **12**(3), p. 465 (2019).
3. Rasouli, E., Basirun, W.J., Rezayi, M., et al. "Ultrasmall superparamagnetic Fe_3O_4 nanoparticles: honey-based green and facile synthesis and in vitro viability assay", *Int. J. Nanomed.*, **13**, pp. 6903-6911 (2018).
4. Nishio, K., Ikeda, M., Gokon, N., et al. "Preparation of size-controlled (30-100 nm) magnetite nanoparticles for biomedical applications", *J. Magn. Magn. Mater.*, **310**, pp. 2408-2410 (2007).
5. Cao, D., Li, H., Pan, L., et al. "High saturation magnetization of ŏ3b3-Fe2O3 nano-particles by a facile one-step synthesis approach", *Sci. Rep.*, **6**, p. 32360 (2016).
6. Onar, K. and Yakinci, M.E. "Synthesis of Fe_3O_4 nanoparticles for biomedical applications", *J. Phys.: Conf. Ser.*, **667**, p. 012005 (2016).
7. Rahmawati, R., Taufiq, A., Sunaryono, S., et al. "Synthesis of magnetite (Fe_3O_4) nanoparticles from iron sands by coprecipitation-ultrasonic irradiation methods", *J. Mater. Environ. Sci.*, **9**(3), pp. 155-160 (2018).
8. Fatima, H., Lee, D.W., Yun, H.J., et al. "Shape-controlled synthesis of magnetic Fe_3O_4 nanoparticles with different iron precursors and capping agents", *RSC Adv.*, **8**(41), p. 22917 (2018).
9. Dutta, B., Shetake, N., Gawali, S.L., et al. "PEG mediated shape-selective synthesis of cubic Fe_3O_4 nanoparticles for cancer therapeutics", *J. Alloys Compd.*, **737**, pp. 347-355 (2018).
10. Iranmanesh, P., Saeednia, S., Mehran, M., et al. "Modified structural and magnetic properties of nanocrystalline $MnFe_2O_4$ by pH in capping agent free co-precipitation method", *J. Magn. Magn. Mater.*, **425**, pp. 31-36 (2017).
11. Yan, J., Mo, S., Nie, J., et al. "Hydrothermal synthesis of monodisperse Fe_3O_4 nanoparticles based on modulation of tartaric acid", *Colloids Surf. A*, **340**(13), pp. 109-114 (2009).
12. Mascolo, M.C., Pei, Y., and Ring, T.A. "Room temperature co-precipitation synthesis of magnetite nanoparticles in a large pH window with different bases", *Materials*, **6**(12), pp. 5549-5567 (2013).
13. Liu, X.D., Chen, H., Liu, S.S., et al. "Hydrothermal synthesis of superparamagnetic Fe_3O_4 nanoparticles with ionic liquids as stabilizer", *Mater. Res. Bull.*, **62**, pp. 217-221 (2015).
14. Karami, H. "Synthesis and characterization of iron oxide nanoparticles by solid state chemical reaction method", *J. Clust. Sci.*, **21**, pp. 11-20 (2010).
15. Dhivya, S.M., Sathiya, S.M., Manivannan, G., et al. "A comparative study on the biopolymer functionalized iron oxide nanocomposite for antimicrobial activity", *Science Direct.*, **3**(10), pp. 3866-3871 (2016).
16. Chaki, S.H., Malek, T.J., Chaudhary, M.D., et al. "Magnetite Fe_3O_4 nanoparticles synthesis by wet chemical reduction and their characterization", *Adv. Nat. Sci.: Nanosci. Nanotechnol.*, **6**(3), p. 035009 (2015).
17. Khoshnevisan, K., Barkhi, M., Zare, D., et al. "Preparation and characterization of CTAB-coated Fe_3O_4 nanoparticles", *Nano-Metal Chemistry*, pp. 644-648 (2012).
18. Wei, Y., Han, B., Hu, X., et al. "Synthesis of Fe_3O_4 nanoparticles and their magnetic properties", *Procedia Eng.*, **27**, pp. 632-637 (2012).
19. Wei, C., Yiran, M., Wei, Z., et al. "One-pot hydrothermal synthesis of rGO-Fe_3O_4 hybrid nanocomposite for removal of Pb(II) via magnetic separation", *Chem. Res. Chin. Univ.*, **31**(4), pp. 508-513 (2015).
20. Dargahzadeh, M., Molaei, M., and Karimipour, M. "Completely quenching of the trap states emission of CdSe QDs by CdS/ZnS shell growth using a one pot photochemical approach and application for dye photodegradation", *J. Lumin.*, **203**, pp. 723-729 (2018).
21. Yanez-Vilar, S., Sanchez, M., Gomez-Aguirre, C., et al. "A simple solvothermal synthesis of MFe_2O_4 (M 1/4 Mn, Co and Ni) nanoparticles", *J. Solid State Chem.*, **182**(10), pp. 2685-2690 (2009).
22. Flores, A.G., Raposo, V., Iniguez, J., et al. "Ferromagnetic resonance in bulk and microparticle samples of $Mn1.3Fe_{17}O_4$", *Phys. Status Solidi.*, **187**, pp. 521-527 (2001).
23. Unni, M., Uhl, A.M., Savliwala, S., et al. "Thermal decomposition synthesis of iron oxide nanoparticles with diminished magnetic dead layer by controlled addition of oxygen", *ACS Nano.*, **11**(2), pp. 2284-2303 (2017).
24. Madhuvilakku, R., Alagar, S., Mariappan, R., et al. "Green one-pot synthesis of flowers-like Fe_3O_4/rGO hybrid nanocomposites for effective electrochemical detection of riboflavin and low-cost supercapacitor applications", *Sens. Actuators, B.*, **253**, pp. 879-892 (2017).
25. Yaacob, I., Nunes, A., Bose, A., et al. "Synthesis and characterization of magnetic nanoparticles in spontaneously generated vesicles", *J. Colloide Interface Sci.*, **168**(34), pp. 289-301 (1994).
26. Ahmadi, S., Chia, C.H., Zakaria, S., et al. "Synthesis of Fe_3O_4 nanocrystals using hydrothermal approach", *J. Magn. Magn. Mater.*, **324**(24), pp. 4147-4150 (2012).
27. Sarkar, Z.K. and Sarkar, F.K. "Synthesis and magnetic properties investigations of Fe_3O_4 nanoparticles", *Int. J. Nanosci. Nanotechnol.*, **7**, pp. 197-200 (2011).

28. Behrad, F., Farimani, M.H.R., Shahtahmasebi, N., et al. "Synthesis and characterization of Fe_3O_4/TiO_2 magnetic and photocatalyst bifunctional core-shell with superparamagnetic performance", *Eur. Phys. J. Plus*, **7**, pp. 130-144 (2015).
29. Andrzejewski, B., Bednarski, W., Kazmierczak, M., et al. "Magnetization enhancement in magnetite nanoparticles capped with alginic acid", *Composites, Part B*, **64**, pp. 147-154 (2014).
30. Iranmanesh, P. Tabatabai Yazdi, Sh. Mehran, M., et al. "Superior magnetic properties of Ni ferrite nanoparticles synthesized by capping agent-free one-step coprecipitation route at different pH values", *J. Magn. Magn. Mater.*, **449**, pp. 172-179 (2018).

Biographies

Masoud Karimipour began his academic career in 2011 in the Department of Physics at Vali-E-Asr University of Rafsanjan, Rafsanjan, Iran, and became an Associate Professor in 2016. He earned his PhD in Solid-state Physics from Ferdowsi University of Mashhad, Mashhad, Iran, in 2011. He did his dissertation entitled "Preparation of room temperature ferromagnetic nanoparticles and thin films based on nonmagnetic materials for spintronic applications and study of their structural, optical and magnetic properties" under the supervision of Prof. Nasser Shahtahmasebi. He is nowadays concerned with the preparation of nanomaterials for biosensors, hydrogen generation, and energy storage in solar cells.

Nafiseh Moradi obtained her MSc degree in Solid-state Physics in 2017 focusing on the synthesis of Ag_2S quantum dots using a microwave method under the supervision of Dr. Masoud Karimipour. Afterwards, she was an assistant researcher at Vali-e-Asr University for 6 months working on the synthesis of iron oxide nanoparticles from waste soil.

Mehdi Molaei began his academic career in 2011 in the Department of Physics at Vali-E-Asr University of Rafsanjan, Rafsanjan, Iran, and became an Associate Professor in 2016. He earned his PhD in Solid-state Physics from Tarbiat Modarres University, Iran, in 2011. He is a specialist in the synthesis of different types of quantum dots and core-shell structures for luminescence in LED and solar cell applications. His major research concern is development of new and facile methods for large-scale production of nanomaterials.

Marzieh Dargahzadeh obtained her MSc in Nanophysics from Vali-E-Asr University of Rafsanjan, Rafsanjan, Iran, in 2018. She did her MSc thesis entitled "Improvement of luminescence properties of CdSe nanoparticles with growth of two shell CdS/ZnS" under the supervision of Dr. Mehdi Molaei. She received a BSc in Meteorology Physics in 2015 from Hormozgan University, Bandar Abbas, Iran. She was an Assistant Researcher at Vali-e-Asr University in 2018 working on water desalination and hydrogen production with Fe_3O_4-reduced graphene oxide nanocomposites.